

Title	Simultaneous phenomenon of particle deposition and reentrainment in charged aerosol flow -- effects of particle charge and external electric field on the deposition layer
Author(s)	Adhiwidjaja, Indra; Matsusaka, Shuji; Yabe, Susumu; Masuda, Hiroaki
Citation	Advanced Powder Technology (2000), 11(2): 221-233
Issue Date	2000
URL	http://hdl.handle.net/2433/198910
Right	© Brill.
Type	Journal Article
Textversion	author

Simultaneous phenomenon of particle deposition and reentrainment in charged aerosol flow

—effects of particle charge and external electric field on deposition layer—

Indra ADHIWIDJAJA, Shuji MATSUSAKA, Susumu YABE and Hiroaki MASUDA

ABSTRACT

Formation of particle deposition layer has been investigated as a simultaneous phenomenon of particle deposition and reentrainment in a turbulent aerosol flow. Aerosol particles passed through a corona charger were pneumatically transported into a glass tube equipped with a ring-type electrode, and the deposition layers formed on the tube wall in various conditions were quantitatively analyzed with particular attention to the effects of particle charge and external electric field on the deposition layer. The charged particles formed a filmy deposition layer around the electrode being independent of the polarity of particle charge and applied voltage. The mass of deposition layer increased with elapsed time and became constant after an equilibrium state of particle deposition and reentrainment. The time dependence was represented by an exponential equation; the time constant decreased with increasing particle charge and/or applied voltage, and the equilibrium mass of deposition layer increased with the particle charge. Furthermore, it was found that appropriate arrangement of electrodes to control external electric field eliminates the filmy deposition layer.

Key Words: Particle Deposition Layer, Reentrainment, Corona Charge, Electric Field

NOMENCLATURE

c	aerosol particle concentration (kg m^{-3})
D_{p50}	mass median diameter of particles (m)
\bar{u}	average air velocity (m s^{-1})
q/m_p	particle charge to mass ratio (C kg^{-1})
r	radial coordinate (m)
t	elapsed time (s)
V	applied voltage (V)
Δx	distance from an electrode (m)
W/A	mass of particles deposited per unit area based on a filmy deposition layer (kg m^{-2})
$(W/A)^*$	equilibrium mass of particles deposited per unit area (kg m^{-2})
W/A_w	mass of particles deposited per unit area based on a wall surface (kg m^{-2})
z	coordinate in the axial direction (m)
 <i>Greek</i>	
ε	permittivity (F m^{-1})
ρ_p	particle density (kg m^{-3})
τ	time constant (s)
ϕ	electric potential (V)

1. INTRODUCTION

Particle deposition and reentrainment in aerosol pipe flows are fundamental phenomena relating to many aerosol operations such as powder dispersion, size classification, dust collection, particle generation and particle sampling. A number of studies on these phenomena have been carried out; almost all of them treated that particle deposition and reentrainment were independent of each other [1~3], and the simultaneous phenomenon of deposition and reentrainment was analyzed simply by a combination of the two phenomena [4, 5]. However, the simultaneous phenomenon observed in industrial powder processes is more complicated; in the first stage fine particles deposit on a wall surface and form a deposition layer, then aggregate particles are reentrained from the deposition layer, and finally the deposition and reentrainment become in equilibrium. Therefore, to clarify the simultaneous phenomenon, the formation process of the deposition layer and equilibrium states between deposition and reentrainment should be analyzed. From this point of view, we have studied the formation of the particle deposition layers and found several new facts [6-9]. A filmy deposition layer formed at a lower air velocity changed into a striped pattern deposition layer as the air velocity increases, and the thickness and the interval of the striped deposition layers were varied corresponding to the operational conditions. When a powder that kept at a lower humidity was pneumatically transported in a glass tube, filmy deposition layers were randomly formed and sometimes disappeared being independent of a striped pattern deposition layer. Also, filmy deposition layers were formed at the parts of the glass tube fixed to a frame using a different material. These filmy deposition layers were probably formed owing to the electrification of the insulating wall, which is caused by particle collisions with the wall and/or the external electric fields. The validity of the argument could be supported by the following experimental result [7]. When a jacket filled with a conductive aqueous solution was attached on the outside of the glass tube to reduce the charge of the glass wall, the filmy deposition layers successfully disappeared. However, the formation of the filmy deposition layers in electrostatic fields was not studied in detail.

In this paper, positive or negative charge aerosol particles are fed into a glass

tube equipped with a ring-type electrode, and filmy deposition layers formed in electrostatic fields are quantitatively analyzed. In addition, we study a method to prevent the formation of the filmy deposition layers using external electrodes.

2. Experimental apparatus and procedure

Figure 1 shows a schematic diagram of the experimental apparatus. The test powder (fly ash: JIS Z8901 No. 10, MMD: $D_{p50} = 3.0 \mu\text{m}$, particle density: $\rho_p = 2390 \text{ kg m}^{-3}$) was discharged continuously from the ultrasonic vibrating capillary tube of a powder feeder [10], and was dispersed into airflow through two ejectors (Pisco, VHH 12 801J). The aerosol particles can be charged positively or negatively with a corona charger (Sankyo Pio-tech, BCA). Aerosol concentration was kept at $2 \times 10^{-3} \text{ kg m}^{-3}$ to make the particles charge homogeneously. The average air velocity was set at 9.3 m s^{-1} to form typical deposition layers as a result of simultaneous particle deposition and reentrainment and the powder flow rate was kept at 11 mg s^{-1} . In these experimental conditions, the particle charge to mass ratio q/m_p can be controlled in the range from -0.01 to $+0.01 \text{ C kg}^{-1}$ by the corona charger.

At a test section, a removable glass tube with 8.6 mm inner diameter and 200 mm long was installed, and two glass tubes 500 mm long and 100 mm long (Fig. 1) with the uniform diameter were connected at the front and the behind, respectively. A ring-type electrode was attached around the glass tube and electric potential was applied in the range from -5 to $+5 \text{ kV}$. The mass of particles deposited was measured using an electric balance after removing the glass tube and the specific charge of aerosol particles was measured using a vacuum-type Faraday cage.

The test powder was dried at $110 \text{ }^\circ\text{C}$ over 12 hours and cooled down in a desiccator at room temperature. Then the experiments were conducted using airflow kept at a relative humidity of 10%.

3. RESULTS AND DISCUSSION

3.1 State of particle deposition layer

Figure 2 shows the photographs of particle deposition layers formed in the glass tube. The background of the glass tube is black, thus the deposited particles look white. As there is no external electrode, filmy deposition layers were randomly formed in addition to a striped pattern deposition layer (Fig. 2(a)). These filmy deposition layers probably result from the electrification of the glass wall caused by collision of particles; namely, non-uniform electric fields were formed around the charged wall. The fields partially enhanced the particle deposition, and consequently the filmy deposition layers were formed. Figures 2(b) and 2(c) show the results for the glass tube equipped with an external electrode made of a copper wire 0.4 mm in diameter. Applied voltage was 5 kV and the specific charge of aerosol particles was $+4.0 \times 10^{-3} \text{ C kg}^{-1}$ (Fig. 2(b)) and $-4.0 \times 10^{-3} \text{ C kg}^{-1}$ (Fig. 2(c)). In both the cases, a filmy deposition layer was formed around the electrode being independent of the polarity of particle charge. In addition, a small amount of filmy deposition layers were formed randomly away from the electrode.

3.2 Time dependence of the amount of a filmy deposition layer

Figure 3 shows the mass of particles deposited per unit area W/A around the external electrode. All the data were obtained from separate experiments; the mass and the area of the filmy deposition layer were measured after carefully wiping the surrounding unnecessary particles deposited in the glass tube at every experiment. First, an experiment was conducted at a constant applied voltage of -5 kV as a parameter of the particle charge to mass ratio (Fig. 3(a)). The mass of particles deposited increases immediately at the beginning of the operation, but the increase does not continue as aggregate particles are reentrained more readily with an increase in the amount of particles deposited. Consequently, particle deposition and reentrainment attains equilibrium; the equilibrium mass increases with the particle charge. The amount of the deposition layer is controlled by both particle adhesive force and aerodynamic separation force. However, the separation force here was constant because the air velocity was not changed in this experiment. Hence, the variation of the equilibrium

mass is ascribed to the adhesive force caused by static electricity. The adhesive force consists of particle-wall image force and electrostatic field forces arising from the applied voltage and/or charged aerosol particles. If particles are accumulated in the deposition layer, additional force caused by particle polarization arises [11]. Figure 3(a) also shows that the time to reach an equilibrium state tends to decrease as the particle charge increases. This is because the electrostatic force enhances the particle deposition [12, 13].

Figure 3(b) shows the results under a constant particle charge. It can be observed that the values of equilibrium mass are almost the same irrespective of the applied voltage. However, the time to reach an equilibrium state decreases with an increase in the applied voltage. This is because the deposition velocity of aerosols increases with the strength of external electric field. Even if no voltage is applied, a filmy deposition layer is formed around the electrode because the existence of the grounded ring-type electrode enhances the electric field, i.e., electric field is concentrated.

Although both the time to reach an equilibrium state and the equilibrium mass for the filmy deposition layer depend on the operational conditions, there is a common feature in the time dependence of the mass of particles deposited. This is also similar to that for a striped pattern deposition layer [9]. Thus, we adopt the same method to analyze the time dependence for the filmy deposition layer. On the assumption that the mass of particles deposited per unit area and unit time $d(W/A)/dt$ is proportional to the difference between real and equilibrium mass of particles deposited, the following equation is derived:

$$\frac{d(W/A)}{dt} = \frac{1}{\tau} \left\{ \left(\frac{W}{A} \right)^* - \frac{W}{A} \right\}, \quad (1)$$

where τ is a time constant, $(W/A)^*$ is the equilibrium mass of particles deposited per unit area. The solution of Eq. (1) can be written as follows:

$$\frac{W}{A} = \left(\frac{W}{A} \right)^* \left\{ 1 - \exp\left(-\frac{t}{\tau} \right) \right\} \quad (2)$$

The solid lines in Fig. 3 are calculated using Eq. (2). The experimental results agree with the calculated ones, hence the time dependence of the mass for a filmy deposition

layer can be also represented by an exponential equation. The values of time constant τ and the equilibrium mass $(W/A)^*$ used for the calculation are summarized in Table 1. It is obvious that the value of τ decreases with increasing particle charge and/or absolute value of applied voltage, and $(W/A)^*$ increases with particle charge.

3.3 Effects of particle charge and applied voltage on the formation of filmy deposition layer

Figure 4 shows the profiles of the amount of particles deposited after the operation at an applied voltage of -5 kV for 40 minutes. The mass of particles deposited per unit area W/A_w is divided into five sections. Although the profile depends on the experimental conditions, the particles deposit mainly at the center where the ring-type electrode is equipped, and the amount of the particles increases with the particle charge. Hence, it is found that the particle deposition is enhanced by the particle charge and the electric field around the ring-type electrode. Figure 5 shows the relationship between the amount of particles deposited W/A_w at the center and the particle charge q/m_p . The amount of particles was not influenced even when the applied voltage varied from -2 kV to -5 kV but it increases with the particle charge. It is of interest to note that the amount of the particles increases even if the polarity of the particle charge is the same as that of the electrode. This fact could also be found in Fig 2(b) and (c). Considering the circumstances mentioned above, the following features are deduced; the position and the velocity of particle deposition are mainly controlled by the external electric field, while adhesive force (image force) of the particles deposited are controlled by the particle charge. As a result, a filmy deposition layer was formed. This is independent of the polarity of particle charge. Since the image force is enhanced with an increase in the amount of particles deposited [14], the filmy deposition layer grows further.

3.4 Reduction of filmy deposition layers using external electrodes

Experiments using a wide electrode made of aluminum foil showed that the filmy

deposition layers were not formed inside the electrode. However, at the end of the electrode, a filmy deposition layer was formed, which was similar to that for the ring-type electrode mentioned above. Figure 6 shows a typical result for particle deposition layers formed in the glass tube equipped with an electrode of 40 mm wide. The electrode was, here, removed for the photography. As the electric potential of the glass wall covered by the wide electrode is almost constant, the strength of the electric field seems to be quite weak. However, at the end of the electrode, the non-uniform electric field is rather strong and a filmy deposition layer is formed there.

Furthermore, we conducted the experiments using narrow electrodes of 3 mm wide, which were attached in different arrangement. The results for the deposition layers in the glass tube are shown in Fig. 7. In the ring-type electrodes arranged at regular intervals, filmy deposition layers were not formed although striped deposition layers were formed (Fig. 7(a)). Also, in an electrode arranged in a spiral, there were no filmy deposition layers observed (Fig. 7(b)).

3.5 Calculation of the electric field in a glass tube.

We calculated the electric fields around an electrode by a computer. To solve the electric field, the following Laplace's equation was adopted.

$$\text{div} (\varepsilon \text{grad } \phi) = 0 \quad (3)$$

where ε is the dielectric constant, ϕ is the electric potential. The values used for the calculation corresponds to the experimental conditions; the inside diameter of the tube is 8.6 mm, outside diameter is 11 mm, the width of the electrode is 3 mm, and the dielectric constant of the tube is 4. The calculation domain is the axial symmetry of 205.5 mm in radius (r) and ± 200 mm long (z), and the electrode is arranged at the center ($z = 0$). The mesh for numerical simulation is $97 (r) \times 122 (z)$. The minimum mesh size near the electrode is $10 \mu\text{m} (r) \times 50 \mu\text{m} (z)$. The boundary conditions are as follows:

$$\phi|_{\text{electrode}} = 5 \text{ kV}, \quad \phi|_{r=205.5 \text{ mm}} = 0$$

$$\phi|_{z=\pm 200 \text{ mm}} = 0, \quad \frac{\partial \phi}{\partial r}|_{r=0} = 0$$

Figure 8 shows the vector and equi-potential diagram of the electric field around the ring-type electrode. To illustrate the electric field in the glass tube, the scale of the radial direction is enlarged more than that of the axial direction—consequently, the vector of the electric field and the equi-potential line do not cross at right angles. The vector of the electric field near the electrode points toward the center of the tube, while at several millimeters up or down from the electrode, the direction of the vector changes to the tube wall. If the applied voltage is negative, the electric field changes into the counter direction of this figure. When the polarity of the particle charge is opposite to the applied voltage, the aerosol particles move toward the electrode and form a filmy deposition layer on the wall near the electrode. On the other hand, when the charged particles and the electrode have the same polarity, the aerosol particles are attracted to the wall a little away from the electrode and deposit there. Since the image force increases with the amount of particles deposited, a filmy deposition layer grows larger and covers the wall near the electrode. Similar filmy deposition layers are also formed and these are independent of the electric polarity. Further, gradient force arising from a non-uniform electric field move the charged aerosol particles toward the electrode but the effect is rather small [15].

Figure 9 shows the calculated results for the electric field in the glass tube equipped with five electrodes of 3 mm wide arranged at regular intervals. Although the strength of the electric field near both ends of a series of electrodes is larger, the strength around other three electrodes is quite small because the neighboring electrodes cancel out the electric potential. In general, the collisions of aerosol particles with an insulator electrify the wall non-uniformly. However, appropriate arrangement of external electrodes enables to reduce the electric field strength and eliminate the filmy deposition layers.

4. CONCLUSIONS

Charged aerosol particles were pneumatically transported into a glass tube equipped with an external electrode, then an experimental study was conducted on the deposition layers formed as a result of a simultaneous phenomenon of particle deposition and reentrainment. The results obtained are summarized as follows:

- 1) Charged aerosol particles form a filmy deposition layer as well as a striped pattern deposition layer, and the electric field near the wall controls the position of the filmy deposition layer.
- 2) Although the filmy deposition layer grows with elapsed time, the growth does not continue as the particle reentrainment occurs more readily with an increase in the amount of particles deposited per unit area. Consequently, the particle deposition and reentrainment reach an equilibrium state. The time dependence of the mass of particles deposited can be represented by an exponential equation.
- 3) The time to reach an equilibrium state decreases with increasing particle charge to mass ratio and/or voltage applied to an external electrode. This is because the electrostatic force in the electric field enhances the particle deposition.
- 4) The mass of particles in an equilibrium state increases with the absolute value of the particle charge. This phenomenon is due to the adhesive force arising from the particle charge—the image force.
- 5) Using a wide electrode or arranging narrow electrodes at regular intervals or in a spiral, enable to reduce the electric field strength and eliminate the filmy deposition layers.

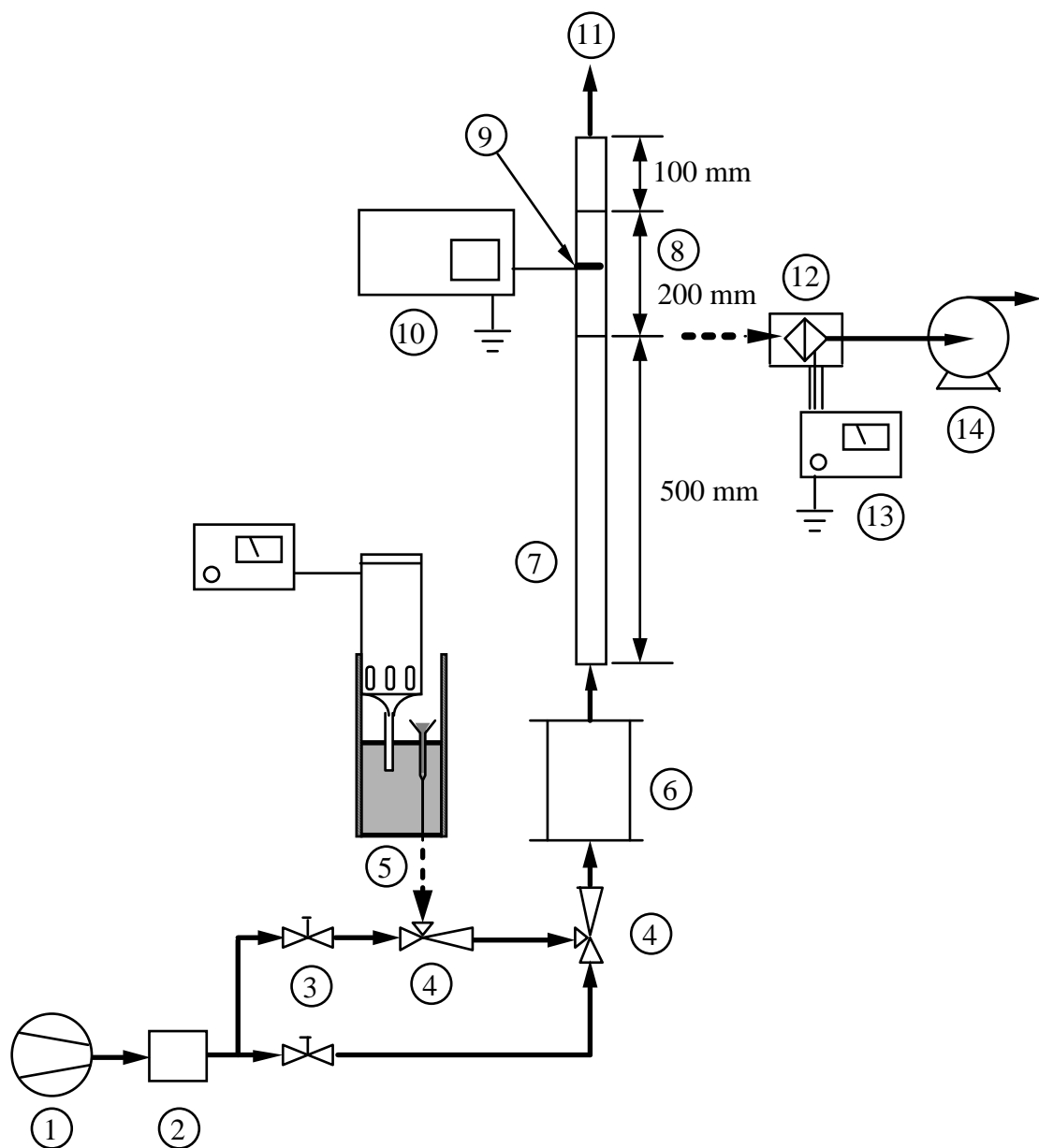
REFERENCES

1. P. G. Papavergos and A. B. Hedley, Particle deposition behaviour from turbulent flows, *Chem. Eng. Res. Des.*, **62**, 275-295 (1984).
2. S. Matsusaka and H. Masuda, Reentrainment phenomena of fine particles, *J. Soc. Powder Technol., Japan*, **29**, 530-538 (1992).
3. G. Ziskind, M. Fichman and C. Gutfinger, Resuspension of particulates from surfaces to turbulent flows –review and analysis, *J. Aerosol Sci.*, **26**, 613-644 (1995).
4. J. W. Cleaver and B. Yates, The effect of re-entrainment on particle deposition, *Chem. Eng. Sci.*, **31**, 147-151 (1976).
5. M. W. Reeks and D. Hall, Deposition and reentrainment of gas-borne particles in recirculating turbulent flows, *J. Fluids Eng.*, **110**, 165-171 (1988).
6. S. Matsusaka, M. Shimizu and H. Masuda, Formation of wall particle layers by simultaneous deposition and reentrainment of fine particles in turbulent aerosol flows, *Kagaku Kogaku Ronbunshu*, **19**, 251-257 (1993).
7. I. Adhiwidjaja, S. Matsusaka and H. Masuda, Mechanism of formation of particle deposition layers by an aerosol flow, *Kagaku Kogaku Ronbunshu*, **22**, 127-133 (1996).
8. I. Adhiwidjaja, S. Matsusaka, T. Hamamura and H. Masuda, The effect of particle size on the movement of a striped pattern deposition layer in an aerosol flow, *J. Soc. Powder Technol., Japan*, **34**, 913-918 (1997).
9. S. Matsusaka, I. Adhiwidjaja, T. Nishio and H. Masuda, Formation of striped pattern deposition layers by an aerosol flow –analysis of thickness and interval of layers", *Advanced Powder Technol.*, **9**, 207-218 (1998).
10. S. Matsusaka, M. Urakawa and H. Masuda, Micro-feeding of fine powders using a capillary tube with ultrasonic vibration, *Advanced Powder Technol.*, **6**, 283-293 (1995).
11. S. Ikumi, H. Mori and H. Masuda, Surface profile and internal structure of particle bed formed by deposition of aerosol particles, *Kagaku Kogaku Ronbunshu*, **12**, 382-387 (1986).
12. H. Masuda and S. Ikumi, Deposition of charged aerosol particles flowing in a cylindrical tube, *J. Soc. Powder Technol., Japan*, **18**, 867-872 (1981).
13. I. B. Wilson, The deposition of charged particles in tubes, with reference to the retention of therapeutic aerosols in the human lung, *J. Colloid Sci.*, **2**, 271-276 (1947).

14. T. B. Jones, *Electromechanics of Particles*, pp. 196-203, Cambridge University Press (1995).
15. The Institute of Electrostatics Japan (ed.), *Handbook of Electrostatics*, pp.1195-1196, Ohmsha (1998).

Table 1 Experimentally Obtained τ and $(W/A)^*$

V (kV)	q/m_p (mC kg ⁻¹)	τ (s)	$(W/A)^*$ (kg m ⁻²)
-5	1.4	1500	0.025
-5	6.7	500	0.043
-5	10.0	450	0.060
0	5.1	2000	0.040
-2	5.1	700	0.040
-5	5.1	500	0.040



- | | |
|-----------------|-----------------------------|
| ① Compressor | ⑧ Glass tube (Test section) |
| ② Dryer | ⑨ Electrode |
| ③ Valve | ⑩ Power voltage supply |
| ④ Ejector | ⑪ Bag filter |
| ⑤ Powder feeder | ⑫ Faraday cage |
| ⑥ Boxer charger | ⑬ Electrometer |
| ⑦ Glass tube | ⑭ Blower |

Fig. 1 Experimental apparatus

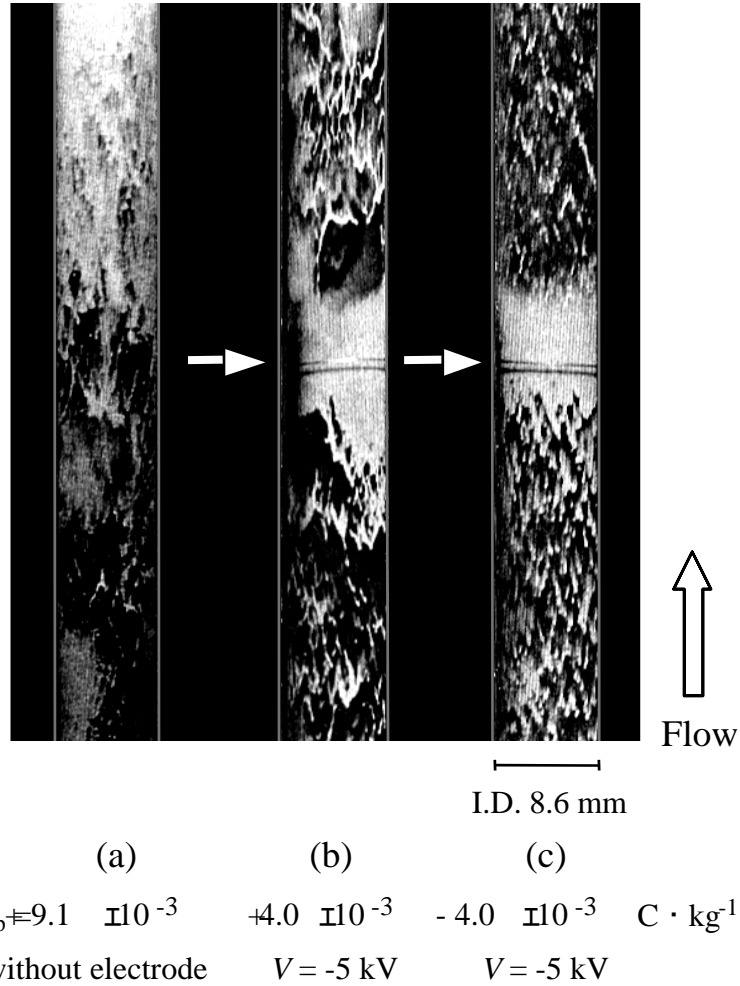


Fig. 2 Particle deposition layers formed in a glass tube (Fly ash No. 10, $D_{p50} = 3.0 \mu\text{m}$, $c = 0.002 \text{ kg} \cdot \text{m}^{-3}$, $\bar{u} = 9.3 \text{ m} \cdot \text{s}^{-1}$, $t = 2400 \text{ s}$)

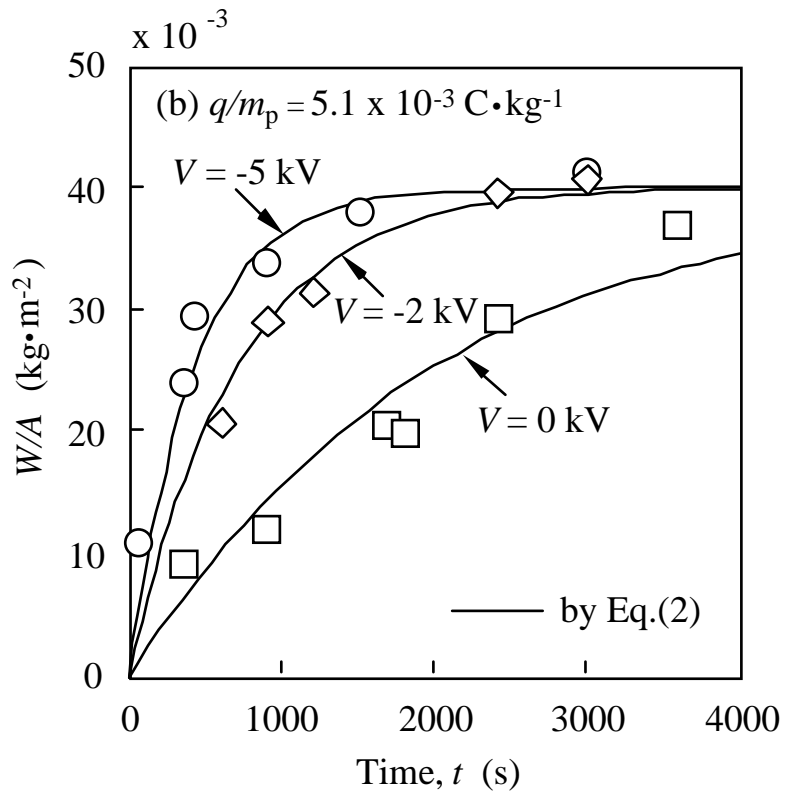
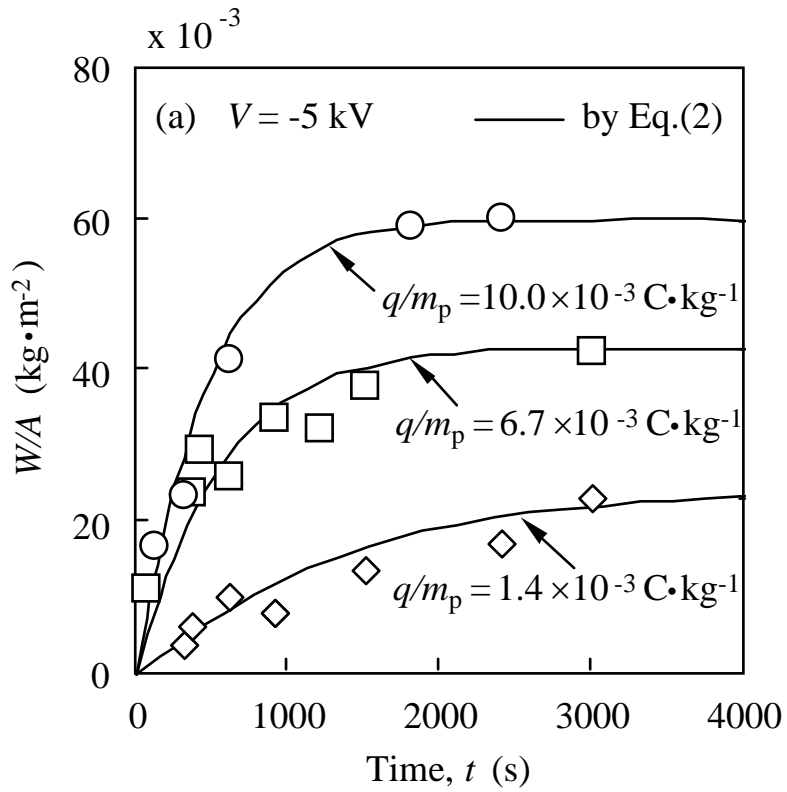


Fig. 3 The mass of particles deposited per unit area (W/A) as a function of time elapsed ($D_{p50} = 3.0 \text{ }\mu\text{m}$, $c = 0.002 \text{ kg}\cdot\text{m}^{-3}$, $\bar{u} = 9.3 \text{ m}\cdot\text{s}^{-1}$)

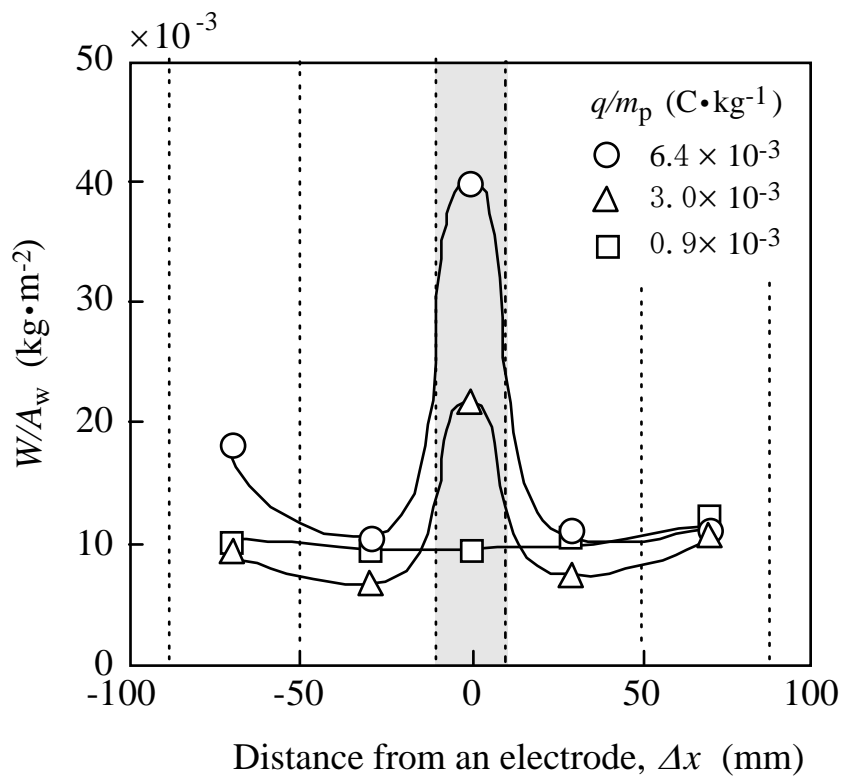


Fig. 4 The mass of particles deposited per unit area W/A_w in each section of test tube ($V = -5 \text{ kV}$, $D_{p50} = 3.0 \text{ }\mu\text{m}$, $c = 0.002 \text{ kg}\cdot\text{m}^{-3}$, $\bar{u} = 9.3 \text{ m}\cdot\text{s}^{-1}$, $t = 2400 \text{ s}$)

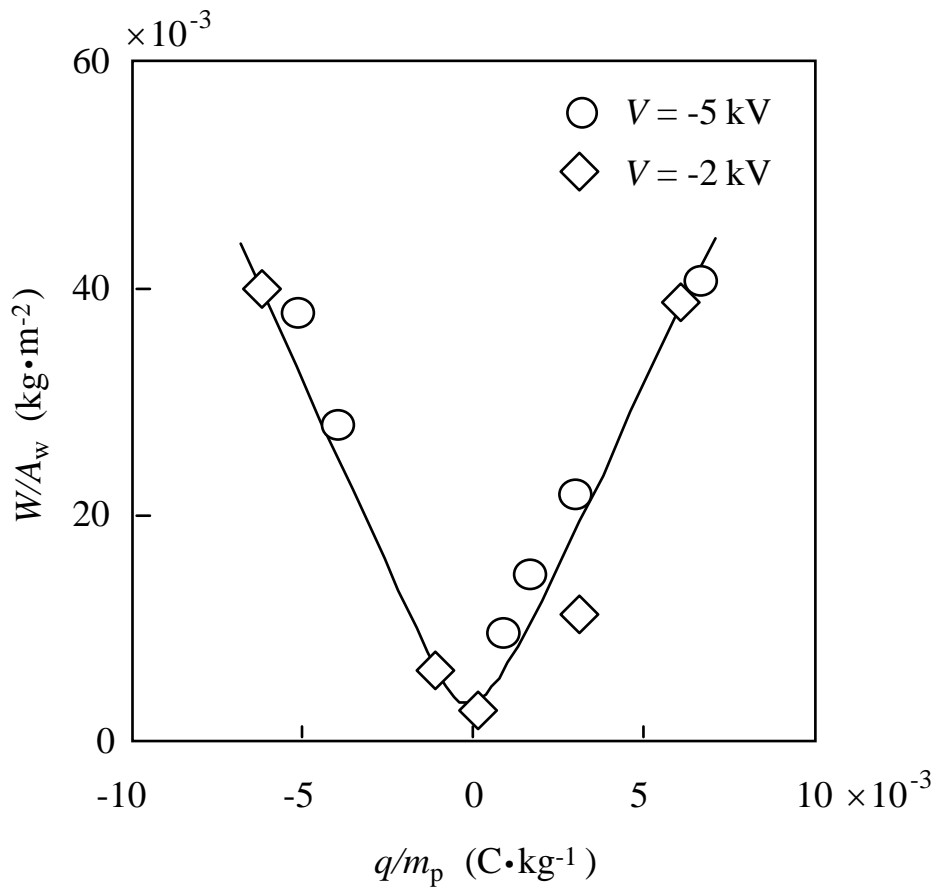


Fig. 5 The mass of particles deposited per unit area W/A_w in the section with an electrode ($D_{p50} = 3.0 \mu\text{m}$, $c = 0.002 \text{ kg} \cdot \text{m}^{-3}$, $\bar{u} = 9.3 \text{ m} \cdot \text{s}^{-1}$, $t = 2400 \text{ s}$)

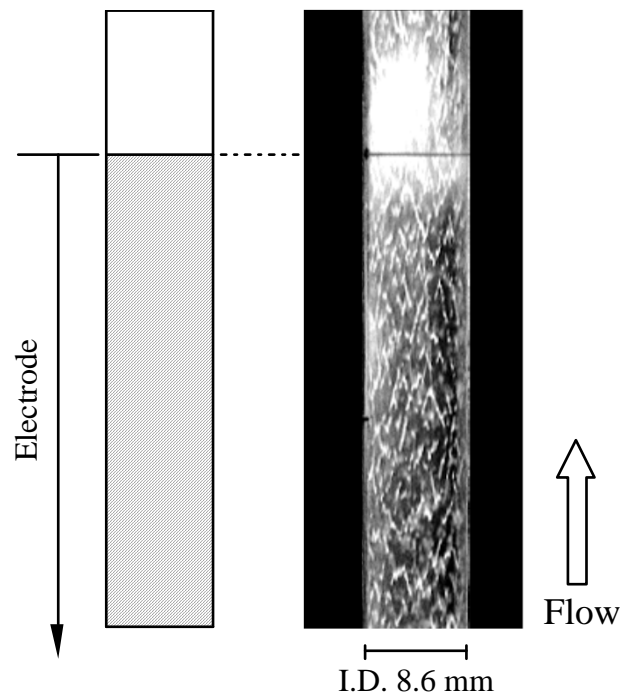
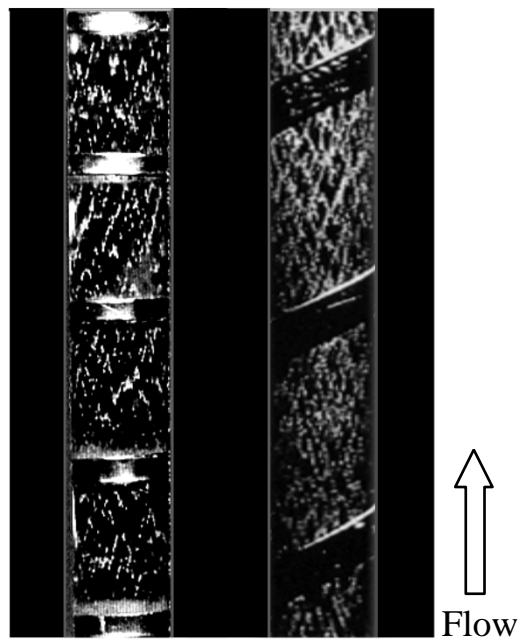


Fig. 6 Effect of a wide electrode on particle deposition layer
(Fly ash No. 10, $D_{p50} = 3.0 \mu\text{m}$, $c = 0.002 \text{ kg} \cdot \text{m}^{-3}$,
 $\bar{u} = 9.3 \text{ m} \cdot \text{s}^{-1}$, $q/m_p = + 3.5 \times 10^{-3}, \text{ C} \cdot \text{kg}^{-1}$, $V = - 5 \text{ kV}$)



I.D. 8.6 mm

(a) multiple electrodes (b) helical electrode
 $q/m_p = +9.1 \times 10^{-3}$ $+6.3 \times 10^{-3} \text{ C} \cdot \text{kg}^{-1}$
 $V = 2 \text{ kV}$ $V = -5 \text{ kV}$

Fig. 7 Formation of deposition layers of striped pattern controlled by different type of electrodes
 (Fly ash No. 10, $D_{p50} = 3.0 \mu\text{m}$, $c = 0.002 \text{ kg} \cdot \text{m}^{-3}$,
 $\bar{u} = 9.3 \text{ m} \cdot \text{s}^{-1}$, $t = 2400 \text{ s}$)

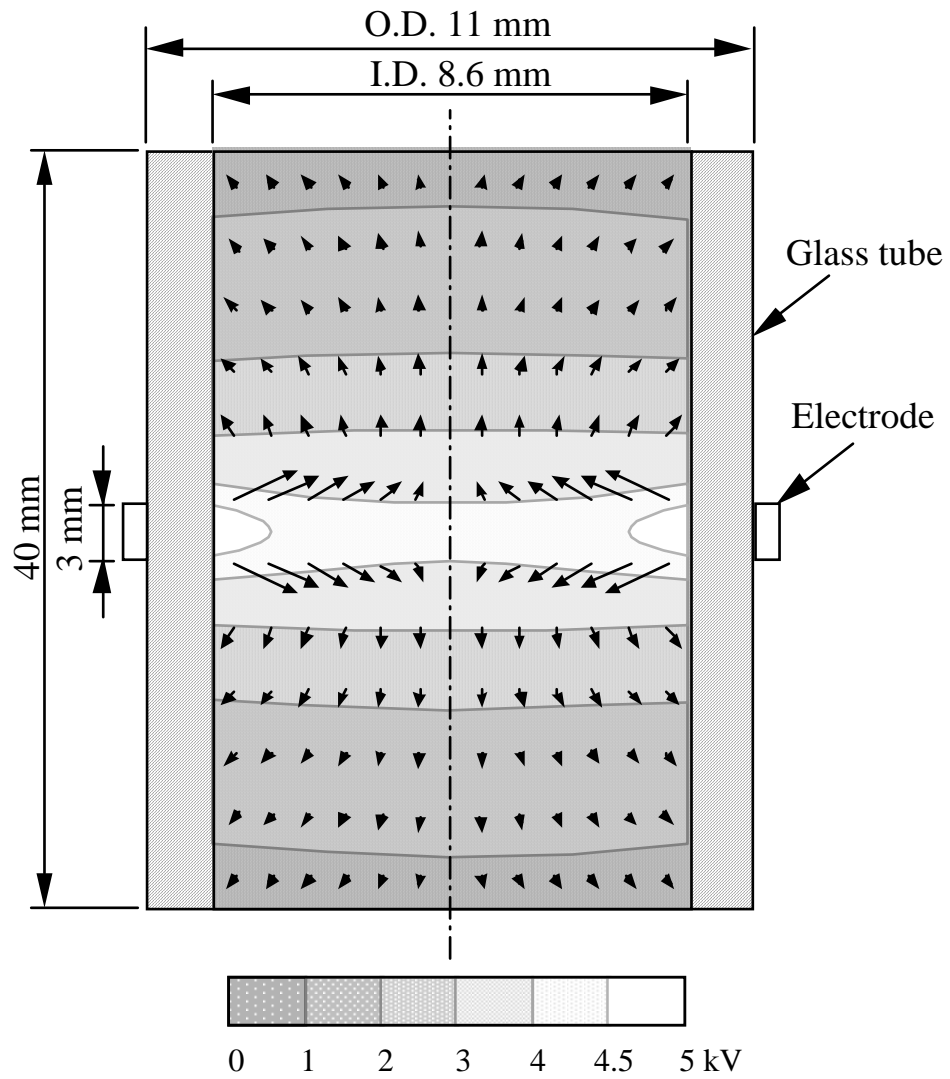


Fig. 8 Calculated electric field near single electrode ($V = 5$ kV)

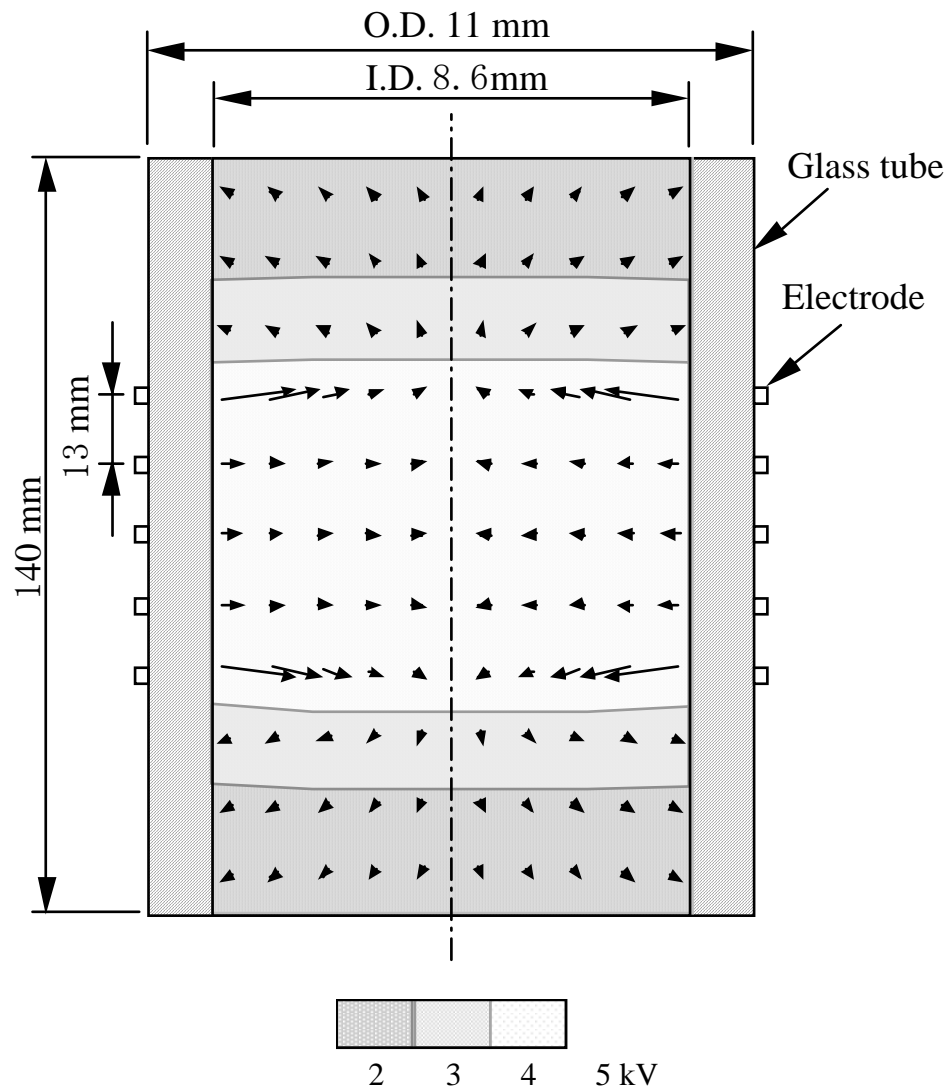


Fig. 9 Calculated electric field near multiple electrodes ($V = 5$ kV)